

Modeling the transmission dynamics of the Middle East Respiratory Syndrome Coronavirus (MERS-CoV) with latent immigrants

S. Usaini¹, A. S. Hassan, S. M. Garba and JM-S. Lubuma

*Department of Mathematics and Applied Mathematics,
University of Pretoria, South Africa.*

Abstract

A new deterministic mathematical model for the transmission dynamics of Middle East Respiratory Syndrome Coronavirus (MERS-CoV) is proposed and fully analyzed. The presented model exhibits a unique endemic equilibrium and there is no infection free equilibrium due to constant influx of latent immigrants. An invasion threshold parameter is derived and stability analysis of the full model and its two special cases is carried out. The impact of quarantine and isolation is assessed via threshold analysis approach, while the impact of immigration on the disease prevalence is discussed. Indeed, we showed that MERS-CoV can be controlled by quick isolation or monitoring close contacts and quarantining of suspected latent immigrants. Further, numerical simulations of the model reveal that the disease can be contained if these preventive measures are combined with high reduction of immigration rate.

Keywords: Middle East Respiratory Syndrome, Isolation, Quarantine.

2010 AMS Subject classification: 34D23, 93C15, 93D20

1 Introduction

Middle East Respiratory Syndrome Coronavirus (MERS-CoV) belongs to the subfamily *Coronavirinae* in lineage C of the genus *Betacoronavirus*. MERS-CoV is one of the four Coronavirus groups of which Severe Acute Respiratory Syndrome (SARS-Cov)

¹Corresponding author: Email address: s3.usaini@gmail.com

belongs [9]. In September 2012, The World Health Organization (WHO), reported the First cases of MERS-CoV [26], a novel respiratory disease, initially localized to Middle East countries. It has a high potential for transmission to close contacts, as observed in communities with sporadic exposure, health care facilities, as well as families having contact with infected members [10]. Coronaviruses are wide spread in Bats around the world but can also be found in many other animal species as well [20]. The first index was reported in Kingdom of Saudi Arabia (KSA) on 13th June, 2012, when unknown coronavirus isolated from a 60yr old man admitted in hospital with a 7 - day history of acute pneumonia, fever, cough, expectoration, short breath and subsequent renal failure which later resulted in fatal outcome [28]. Shortly thereafter, on 14th September, 2012, the United Kingdom Health Protection Agency (HPA) Imported Fever Service was notified of a case of unexplained virus, later named human coronavirus England 1. It has been isolated from another patient with history of severe respiratory illness in an intensive care unit (ICU) of London hospital. The index has been transferred from Qatar and had a history of travel to Saudi Arabia [3]. The origin of the disease was traced back to an earlier time - April, 2012, when health care workers in an ICU of a hospital in Zarqa, Jordan were confirmed to have been contracted with the novel coronavirus [9]. From June, 2012 to 25th September, 2013, WHO reported total of 133 cases with 55 deaths from 9 countries [20]. Up to 14th March, 2014, there were 477 globally reported cases and alerts including additional 7 countries [15]. Globally, from September 2012 to 17th April, 2013, WHO has been informed of a total of 243 laboratory-confirmed cases of infection with MERS-CoV, including 93 deaths [25]. It has been observed that all cases outside Middle East are traced back to the region either by travel to or from the affected areas or by direct or indirect contact with others who have a travel history to Middle East [1].

The epidemiological data available suggest that the infection is primarily zoonotic in nature, with possible cross-species transmission between humans and animals (Bats, Camels). Some of the reasons advanced are: Close phylogenetic similarity between viruses isolated from humans, bats and camels; presence of viral neutralizing antibodies in dromedary camels for the past 2 decades from (EGP, JO, KSA, OM, Canary Island), and none in other livestock [1, 13, 16, 21, 22]; close association between camels and humans as source of food, sporting and as pets. However, most of the reported cases have no close contact with camels or bats . Therefore, the direction of transmission from humans to animals or vice versa, host, reservoir e.t.c. remain unknown [1, 16, 17].

The established clinical symptoms of MERS-CoV include fever, cough, shortness of breath, acute pneumonia, expectoration, hemoptysis often followed by renal failure [2, 20, 28]. Gastrointestinal symptoms like vomiting and diarrhea are also common [2]. The incubation period was estimated to be 5.2–5.5 days and the serial interval (the time between the successive onset of symptoms in a chain of transmission) was 7.6 days [2]. According to Cauchemez *et al*, [7], the estimated basic reproduction number obtained

from all confirmed and probable of human cluster cases from Middle East (up to Aug 8, 2013) and the first 133 cases [20], were in the range 0.8–1.3 and 0.6 respectively. The implication of the former result is that self-sustaining transmission in the absence of control measures may occur. The average age of the first 133 reported MERS-CoV cases was 52 years with male having higher case-fatality risk of 52% compared to women 24% [20].

Clinically, whenever there is an outbreak or re-emergence of new or an old infection in a community/country, in the absence of vaccine or treatment, isolation and quarantine of individuals with clinical symptoms or suspected to be exposed to the pathogens have proved to be effective ways of containing the disease [11, 23]. The World Health Organization is concerned, among others, with the gaps in understanding the degree of transmissibility between people, possibility of "super spreaders" and potential for sustainable person-to-person transmission and spread [10]. However, several mathematical epidemic models incorporating one of such control measures or both exist in the literature, see for instance, [11, 18, 23, 24, 27]. For the 2015 epidemic outbreak of MERS-Cov in the Republic of Korea, two deterministic models for the transmission dynamics of MERS-Cov with and without control measures were developed in [27]. The basic reproduction number, \mathcal{R}_0 was estimated to reach up to 4.422. The numerical analysis reveals that lack of self-protection sense and targeted control measures were the reasons of the outbreak spread quickly. However, it was reported that strengthening self-protection ability of susceptible and quickly isolating or monitoring close contacts are effective measures to control the disease. Furthermore, partial correlation analysis shows that the infectivity and proportion of the asymptomatic infected cases have much influence on the disease spread. In the same vain, another deterministic model was designed to analyze the MERS-CoV outbreak in the Republic of Korea [18]. The proposed model explicitly incorporates superspreading events and time-dependent transmission and isolation rates. The superspreaders are those who transmit the virus to more than 20 patients and have underlying respiratory diseases with a severe cough. The impact of the timing of control measures associated with a reduction of the transmission rate and diagnostic delays on the outbreak size and duration was assessed. It was observed that early interventions within 1 week after the epidemic onset is a promising means to reduce the size and duration of the MERS-CoV epidemic.

In a similar note, an *SEIQJR* - SARS model with both quarantine and isolation strategies was presented in [11]. The analysis of this model reveals that a reduction in the contact rate between susceptible and infected individuals by isolating the latter is a critically important strategy that can control SARS outbreaks with or without quarantine. It was reported that an optimal isolation is more effective than sub-optimal isolation and quarantine together. And that an optimal isolation combined with a highly effective screening programme at the points of entry would lead to a community-wide eradication of SARS.

It is well known that migration and immigration greatly increase the spread of many infectious diseases at a regional, national and global scale [4, 12]. Simple models for disease transmission incorporating immigration of infective individuals was presented in [4]. The models exhibit a single endemic equilibrium that is asymptotically stable. It was revealed that there is no disease free equilibrium in the presence of immigration of infectives. For HIV transmission model a considerable reduction of infectives was suggested by screening and quarantining of infectives. While both immigration/migration terms were incorporated into all sub-population compartments, susceptible and infected, of two types of well-known heterogeneous epidemic models: multistage models and multi-group models for HIV/AIDS and other sexually transmitted diseases (STDs). It was shown that, the disease always becomes endemic in the population and tends to a unique asymptotically stable endemic equilibrium when migration or immigration into infected sub-population is present [12].

In this paper, a disease transmission model for MERS-CoV epidemic incorporating immigration of susceptible and latently infected individuals is proposed to assess the impacts of quarantine and isolation strategies in controlling the disease. As in the previous studies, the main result is that our model exhibit a unique asymptotically stable endemic equilibrium and there is no disease free equilibrium when immigration into latently infected sub-population is present. While such equilibria exist for the case when either all the immigrants are susceptible or the immigration rate is negligible. The impact of quarantine and isolation is assessed in relation to the relative infectiousness of quarantined and isolated individuals. Further, eradication of MERS-CoV is feasible by reduction of immigration rate of latently infected individuals. The proposed model extends in some sense the aforementioned models in the literature as follows:

- (i) In the presented model, demographic features are incorporated and vital mathematical analysis is carried out, while these were not provided in MERS-CoV model proposed in [27].
- (ii) In [18] there were only two sources of infection, here we consider four sources of infection.
- (iii) Although, immigration into both susceptible and infective compartments is common to [4, 12] and our model, in the latter we used saturated incidence formulation when the former used a simple mass action formulation.
- (iv) For the SARS model in [11], quarantined individuals are asymptomatic infectives who develop symptoms and then move to the isolated class. In our model, some quarantined individuals do not show symptoms and become susceptibles while others recovered by either treatment or acquiring natural immunity and move to recovered compartment.

The remaining part of the paper is organized as follows. In section 2, we describe the mathematical model. In section 3, rigorous analysis of the model is provided including its basic properties, existence and stability of the model equilibria, and the impact of quarantine, isolation and immigration rate are discussed. Numerical simulations supporting the theoretical results are provided. In section 4, we provide a concluding remarks.

2 Model formulation

The susceptible human population is generated *via* recruitment by birth (at a constant rate Π) and immigration (at a rate αq); where $0 \leq q \leq 1$ account for the fraction of the inflow of migrants into the community (by air or road) who are susceptible, and by recovery of quarantined individuals at a rate $\sigma(1 - p)$; where $0 < p < 1$ is a fraction of quarantined individuals tested with no clinical symptoms of the disease. This population is decreased following infection with MERS-CoV, which can be acquired *via* effective contact with infectious human (at a rate λ), where

$$\lambda = \frac{\beta(\eta_1 L + I + \eta_2 Q + \eta_3 J)}{N}$$

Here the parameter β is the effective contact rate (contact capable of leading MERS-CoV infection). Furthermore, $0 \leq \eta_1 \leq 1$, $0 \leq \eta_2 \leq 1$ and $0 \leq \eta_3 \leq 1$ are modification parameters accounting for the assumed reduction in infectiousness of individuals in the latent (L), quarantine (Q) and isolated (J) classes, in comparison to infectious individuals in I class. Natural death is assumed to occur in all human compartments at a rate μ . Thus, the rate of change of the susceptible population is given by

$$\frac{dS}{dt} = \Pi + \alpha q + \sigma(1 - p)Q - (\lambda + \mu)S.$$

The population of individuals in the latent class is increased by immigration at the rate $\alpha(1 - q)$ and by infection (at the rate λ), and is decreased by the development of clinical symptoms (at a rate τ_1), quarantine (at a rate τ_2) and natural death, so that

$$\frac{dL}{dt} = \alpha(1 - q) + \lambda S - (\tau_1 + \tau_2 + \mu)L.$$

The population of infectious individuals with clinical symptoms of MERS-CoV in I class increases following the development of clinical symptoms by individuals in latent class (at the rate τ_1). This population is decreased by isolation (at a rate γ), recovery (at a rate δ_1), MERS-CoV induced mortality (at a rate ν_1) and natural death, this gives

$$\frac{dI}{dt} = \tau_1 L - (\gamma + \nu_1 + \delta_1 + \mu)I.$$

The population of quarantine individuals increases following the quarantine of individuals in the latent class (at the rate τ_2). This population is decreased by recovery (at a rate σ) and natural death, so that

$$\frac{dQ}{dt} = \tau_2 L - (\sigma + \mu)Q.$$

The population of individuals that are isolated ($J(t)$) is generated by the isolations of infectious individuals with clinical symptoms of MERS-CoV (at the rate γ). It is decreased by recovery (at a rate δ_2), disease induced death (at a rate ν_2) and natural death. Hence

$$\frac{dJ}{dt} = \gamma I - (\nu_2 + \delta_2 + \mu)J.$$

Finally, the recovered population is generated by the recovery of individuals in I , J and Q classes at the rates δ_1 , δ_2 and σp , respectively, and decrease due to natural death. This gives

$$\frac{dR}{dt} = \delta_1 I + \delta_2 J + \sigma p Q - \mu_B R.$$

In summary, the MERS-CoV transmission model is given by the following system of non-linear differential equations (a flow diagram of the model is given in Figure 1 and the associated variables and parameters are described in Table 1, respectively).

$$\begin{aligned} \frac{dS}{dt} &= \Pi + \alpha q + \sigma(1-p)Q - \frac{\beta(\eta_1 L + I + \eta_2 Q + \eta_3 J)}{N} S - \mu S, \\ \frac{dL}{dt} &= \alpha(1-q) + \frac{\beta(\eta_1 L + I + \eta_2 Q + \eta_3 J)}{N} S - (\tau_1 + \tau_2 + \mu)L, \\ \frac{dI}{dt} &= \tau_1 L - (\gamma + \nu_1 + \delta_1 + \mu)I, \\ \frac{dQ}{dt} &= \tau_2 L - (\sigma + \mu)Q, \\ \frac{dJ}{dt} &= \gamma I - (\nu_2 + \delta_2 + \mu)J, \\ \frac{dR}{dt} &= \delta_1 I + \delta_2 J + \sigma p Q - \mu R, \end{aligned} \tag{1}$$

with nonnegative initial conditions $S(0) \geq 0$, $L(0) \geq 0$, $I(0) \geq 0$, $Q(0) \geq 0$, $J(0) \geq 0$, $R(0) \geq 0$.

Since the last compartment (R) does not appear in the first five equations of model (1), it is convenient to discard the last equation of system (1) for theoretical analysis.

The equation for the total population which is obtained by adding all the equations of (1) is given by

$$\frac{dN(t)}{dt} = \Pi + \alpha - \mu N(t) - \nu_1 I(t) - \nu_2 J(t). \tag{2}$$

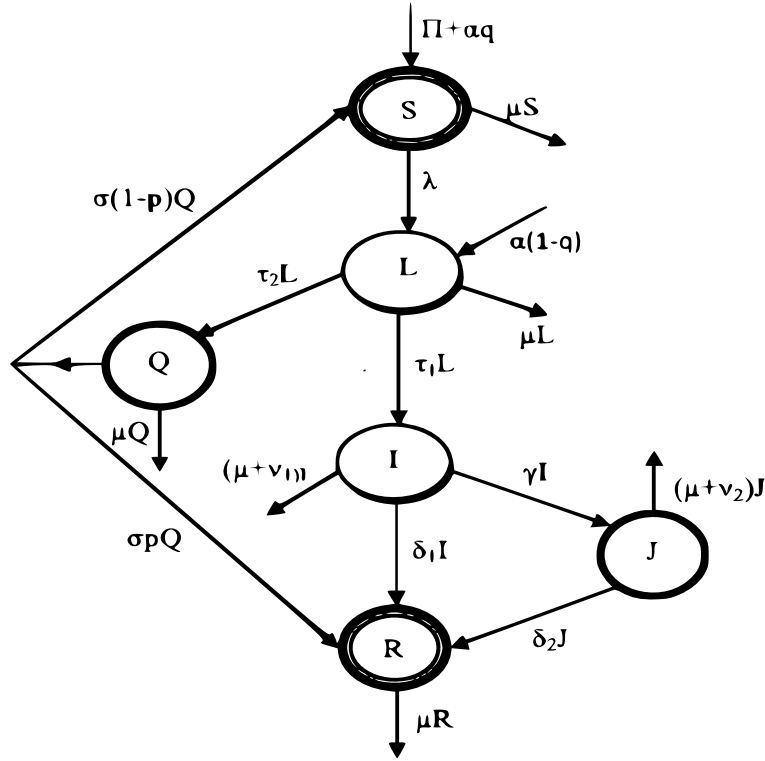


Figure 1: The flow diagram of model (1). The parameter, $\lambda = \frac{\beta(\eta_1 L + I + \eta_2 Q + \eta_3 J)}{N}$.

3 Analysis of model (1)

3.1 Basic properties

The basic properties of the model can now be investigated.

Lemma 1 *The solution $(S(t), L(t), I(t), Q(t), J(t), R(t))$ of model (1) with positive initial conditions, exists for all $t \geq 0$ and is unique. Furthermore, $S(t) > 0$, $L(t) > 0$, $I(t) > 0$, $Q(t) > 0$ and $J(t) > 0$ for all $t \geq 0$.*

Using Lemma 1 on equation (2), we have the following result.

Lemma 2 *The biologically-feasible region of model (1) is*

$$\Gamma = \{(S(t), L(t), I(t), Q(t), J(t), R(t)) \in \mathbb{R}_+^6 : S(t) + L(t) + I(t) + Q(t) + J(t) + R(t) \leq \frac{\Pi + \alpha}{\mu}\}$$

which is positively-invariant and attracting.

Proof. Adding the equations of the model (1) gives

$$\frac{dN(t)}{dt} = \Pi + \alpha - \mu N(t) - \nu_1 I(t) - \nu_2 J(t),$$

Table 1: Description of parameters of model (1)

Parameter	Interpretation
Π	Recruitment rate of susceptible humans by birth
q	Fraction of immigrant humans
α	Recruitment rate of humans by immigration
σ	Removal rate from quarantined
β	Transmission coefficient
η_1, η_2, η_3	Modification parameters for reduction in infectiousness of latent, quarantined & isolated individuals, respectively
μ	Natural death rate in all classes
τ_1, τ_2	Progression rates to infectious/quarantined classes, respectively
γ	Isolation rate
ν_1, ν_2	Disease-induced death rates for infectious and isolated individuals, respectively
δ_1, δ_2	Recovery rates for infectious and isolated individuals, respectively
p	Fraction of quarantined humans

so that

$$\frac{dN(t)}{dt} = \Pi + \alpha - \mu N(t).$$

It follows that $\frac{dN(t)}{dt} \leq 0$ if $N(t) > \frac{\Pi + \alpha}{\mu}$. Thus, a standard comparison theorem can be used to show that

$$N(t) \leq N(0)e^{-\mu t} + \frac{\Pi + \alpha}{\mu} [1 - e^{-\mu t}].$$

In particular, $N(t) \leq \frac{\Pi + \alpha}{\mu}$ if $N(0) \leq \frac{\Pi + \alpha}{\mu}$. Thus Γ is positively invariant. Furthermore, if $N(t) > \frac{\Pi + \alpha}{\mu}$, then either the solution enters Γ in finite time or $N(t)$ approaches $\frac{\Pi + \alpha}{\mu}$ and the infected variables L, I, Q and J approaches zero. Hence, Γ is attracting. That is, all solutions in \mathbb{R}_6^+ eventually enter Γ .

3.2 Existence and stability of equilibria

It should be noted that model (1) has no disease free equilibrium (DFE) due to the constant inflow of newly latent individuals. Let $\hat{\mathcal{E}} = (\hat{S}, \hat{L}, \hat{I}, \hat{Q}, \hat{J})$ be the equilibrium solution of system (1). Then setting the right hand side of (1) to zero we obtain

$$\begin{aligned}
\hat{S} &= \frac{K_1 K_3 (\Pi + \alpha q) + \alpha \sigma \tau_2 (1-p)(1-q)}{(\mu + \hat{\lambda}) [\tau_2 \mu + (\tau_1 + \mu)(\sigma + \mu)] + \tau_2 \sigma (\mu + \hat{\lambda} p)}, \\
\hat{L} &= \frac{K_3 [\hat{\lambda} (\Pi + \alpha) + \mu \alpha (1-q)]}{(\mu + \hat{\lambda}) [\tau_2 \mu + (\tau_1 + \mu)(\sigma + \mu)] + \tau_2 \sigma (\mu + \hat{\lambda} p)}, \\
\hat{I} &= \frac{\tau_1 K_3 [\hat{\lambda} (\Pi + \alpha) + \mu \alpha (1-q)]}{K_2 \{ (\mu + \hat{\lambda}) [\tau_2 \mu + (\tau_1 + \mu)(\sigma + \mu)] + \tau_2 \sigma (\mu + \hat{\lambda} p) \}}, \\
\hat{Q} &= \frac{\tau_2 [\hat{\lambda} (\Pi + \alpha) + \mu \alpha (1-q)]}{(\mu + \hat{\lambda}) [\tau_2 \mu + (\tau_1 + \mu)(\sigma + \mu)] + \tau_2 \sigma (\mu + \hat{\lambda} p)}, \\
\hat{J} &= \frac{\tau_1 \gamma K_3 [\hat{\lambda} (\Pi + \alpha) + \mu \alpha (1-q)]}{K_2 K_4 \{ (\mu + \hat{\lambda}) [\tau_2 \mu + (\tau_1 + \mu)(\sigma + \mu)] + \tau_2 \sigma (\mu + \hat{\lambda} p) \}},
\end{aligned} \tag{3}$$

where $K_1 = \tau_1 + \tau_2 + \mu$, $K_2 = \gamma + \nu_1 + \delta_1 + \mu$, $K_3 = \sigma + \mu$, $K_4 = \nu_2 + \delta_2 + \mu$,

$$\hat{\lambda} = \frac{\beta (\hat{I} + \eta_1 \hat{L} + \eta_2 \hat{Q} + \eta_3 \hat{J})}{\hat{N}} \tag{4}$$

and

$$\hat{N} = \hat{S} + \hat{L} + \hat{I} + \hat{Q} + \hat{J}. \tag{5}$$

Substituting (3) and (5) into equation (4) yields after algebraic manipulations (6).

$$\begin{aligned}
& \frac{\hat{\lambda} \{ K_1 K_3 (\Pi + \alpha q) + \alpha \sigma \tau_2 (1-p)(1-q) \}}{(\mu + \hat{\lambda}) [\tau_2 \mu + (\tau_1 + \mu)(\sigma + \mu)] + \tau_2 \sigma (\mu + \hat{\lambda} p)} + \Phi K_3 (\hat{\lambda} - \eta_1 \beta) \\
& + \Phi \left\{ \frac{\tau_1 K_3 (\hat{\lambda} - \beta)}{K_2} + \tau_2 (\hat{\lambda} - \eta_2 \beta) + \frac{\tau_1 \gamma K_3 (\hat{\lambda} - \eta_3 \beta)}{K_2 K_4} \right\} = 0
\end{aligned} \tag{6}$$

with

$$\Phi = \frac{[\hat{\lambda} (\Pi + \alpha) + \mu \alpha (1-q)]}{(\mu + \hat{\lambda}) [\tau_2 \mu + (\tau_1 + \mu)(\sigma + \mu)] + \tau_2 \sigma (\mu + \hat{\lambda} p)}.$$

Thus, the endemic equilibria of system (1) correspond to the positive values of (3) obtained by using the positive solutions of (6).

We define an invasion threshold by

$$\mathcal{R}_i = \frac{\beta (\Pi + \alpha) [\tau_1 K_3 (K_4 + \eta_3 \gamma) + K_2 K_4 (\eta_1 K_3 + \eta_2 \tau_2)]}{K_1 K_2 K_3 K_4 (\Pi + \alpha q)}. \tag{7}$$

Thus, we obtain the following results.

Theorem 1 *Model (1) has:*

(i) *a unique endemic equilibrium for all values of \mathcal{R}_i if $q \in [0, 1)$ and $\alpha > 0$,*

(ii) a unique endemic equilibrium if $\mathcal{R}_i > 1$ and either $q = 1$ or $\alpha = 0$,

(iii) no endemic equilibrium if $\mathcal{R}_i \leq 1$ and either $q = 1$ or $\alpha = 0$.

Proof. Re-arranging and simplifying equation (6) gives the following quadratic equation for $\hat{\lambda}$

$$a\hat{\lambda}^2 + b\hat{\lambda} + c = 0, \quad (8)$$

where

$$\begin{aligned} a &= (\Pi + \alpha)[K_2K_4(K_3 + \tau_2) + \tau_1K_3(K_4 + \gamma)], \\ b &= \prod_{i=1}^4 K_i(\Pi + \alpha q)(1 - \mathcal{R}_i) + \alpha(1 - q)\mu\{\tau_2K_2[K_4\sigma(1 - p) + K_1\mu] \\ &\quad + K_3K_4\mu(\tau_1 + K_2) + \tau_1K_3\alpha\mu\}, \\ c &= -\alpha\beta\mu^2(1 - q)[K_2K_4(\eta_1K_3 + \eta_2\tau_2) + \tau_1K_3(K_4 + \eta_3\gamma)], \end{aligned} \quad (9)$$

The coefficient a of equation (8) is always positive and c is always negative (noting that $\alpha > 0$ and $q \in (0, 1)$), whereas b is positive if $\mathcal{R}_i \leq 1$. If $\mathcal{R}_i > 1$, b can also be positive or negative. Thus, model (1) has a unique endemic equilibrium for any sign of b by Descartes rule of sign. This proves (i). Next, if $q = 1$ or $\alpha = 0$, then the coefficient $c = 0$ and equation (8) reduces to

$$a\hat{\lambda} + b = 0, \quad (10)$$

with either

$$\begin{aligned} a &= (\Pi + \alpha)[K_2K_4(K_3 + \tau_2) + \tau_1K_3(K_4 + \gamma)], \\ b &= \prod_{j=1}^4 K_j(\Pi + \alpha)(1 - \mathcal{R}_i), \end{aligned} \quad (11)$$

or

$$\begin{aligned} a &= \Pi[K_2K_4(K_3 + \tau_2) + \tau_1K_3(K_4 + \gamma)], \\ b &= \prod_{j=1}^4 K_j\Pi(1 - \mathcal{R}_i), \end{aligned} \quad (12)$$

respectively. It is clear that, in each case the solution $\hat{\lambda} = -\frac{b}{a}$ of (10) is positive if $\mathcal{R}_i > 1$ and negative when $\mathcal{R}_i < 1$. Moreover, for $\mathcal{R}_i = 1$, the coefficient b of (10) is zero and so, the coefficient a of this equation must be zero since $\hat{\lambda}$ cannot be zero. Hence, equation (10) has no solution whenever $\mathcal{R}_i = 1$. Consequently these prove (ii) and (iii). \blacksquare

It follows from (7) that if either $q = 1$ or $\alpha = 0$, then the invasion threshold, \mathcal{R}_i reduces to

$$\mathcal{R}_i^* = \frac{\beta[\tau_1K_3(K_4 + \eta_3\gamma) + K_2K_4(\eta_1K_3 + \eta_2\tau_2)]}{K_1K_2K_3K_4}. \quad (13)$$

The uniqueness of the endemic equilibrium, $\hat{\mathcal{E}}$ allows us to numerically show its global stability as depicted in Figure 2, since the analytical proof is quite involved.

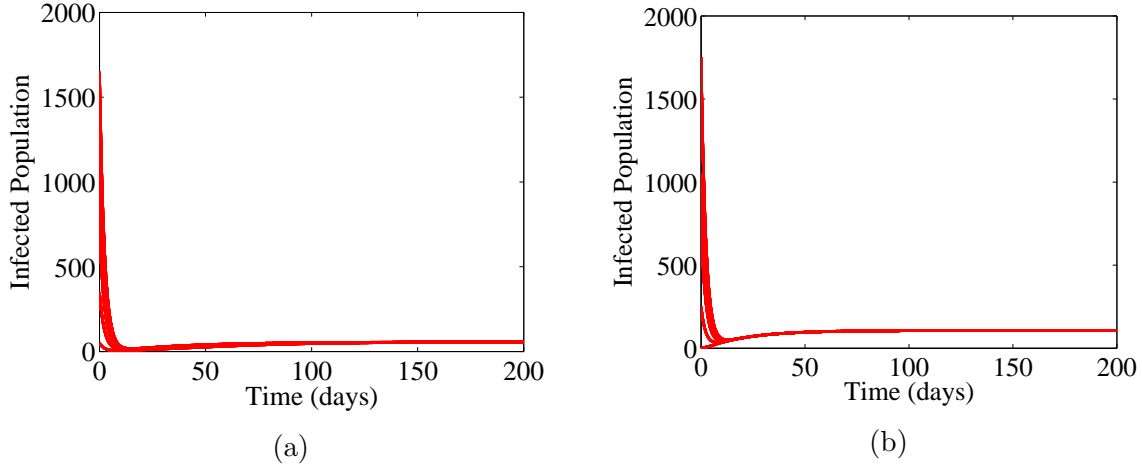


Figure 2: Numerical simulations showing the GAS of endemic equilibrium, $\hat{\mathcal{E}}$ for $\mathcal{R}_i \leq 1$ (a) $q = 0.85$, $\alpha = 400$, $\beta = 0.25$, $\mathcal{R}_i = 0.74$, $\mathcal{R}_i^* = 0.71$ and in (b) $q = 0.52$, $\alpha = 300$, $\beta = 3$, $\mathcal{R}_i = 9.55$, $\mathcal{R}_i^* = 8.49$.

3.3 Immigration cases

As mentioned earlier, when all the immigrants are susceptible, $q = 1$ or the immigration rate is negligible ($\alpha = 0$) the threshold parameter is as defined in (13). Furthermore, for each of such scenarios a disease free equilibrium exists.

For the first case, in the absence of infection, model (1) with $q = 1$ exhibits a locally asymptotically stable disease free equilibrium given by

$$\mathcal{E}_0^q = (S^*, L^*, I^*, Q^*, J^*) = \left(\frac{\Pi + \alpha}{\mu}, 0, 0, 0, 0 \right).$$

In fact, the Jacobian matrix evaluated at \mathcal{E}_0 , denoted by \mathfrak{J}_q is

$$\mathfrak{J}_q = \begin{pmatrix} -\mu & -\beta\eta_1 & \beta & \sigma(1-p) & -\beta\eta_3 \\ 0 & \beta\eta_1 - K_1 & -\beta & \beta\eta_2 & \beta\eta_3 \\ 0 & \tau_1 & -K_2 & 0 & 0 \\ 0 & \tau_2 & 0 & -K_3 & 0 \\ 0 & 0 & \gamma & 0 & -K_4 \end{pmatrix}. \quad (14)$$

The eigenvalues of this matrix are: $-\mu$, and the eigenvalues of the matrix \mathfrak{J}_{q_0} which is obtained by deleting the first/last rows and the first/last columns of \mathfrak{J}_q . Then, the characteristic polynomial of this matrix is

$$\lambda^4 + A\lambda^3 + B\lambda^2 + C\lambda + D = 0, \quad (15)$$

with

$$\begin{aligned} A &= K_1 + K_2 + K_3 + K_4 - \beta\eta_1 \\ B &= K_3K_4 + (K_3 + K_4)(K_1 + K_3 - \beta\eta_1) + K_2(K_1 - \beta\eta_1) - \beta(\tau_1 + \tau_2\eta_2) \\ C &= K_1K_2K_4 \left(1 - \frac{\beta\tau_1(K_4 + \eta_3\gamma)}{K_1K_2K_4} \right) + K_1K_3(K_2 + K_4) \left(1 - \frac{\beta(\eta_1K_3 + \eta_2\tau_2)}{K_1K_3} \right) \\ &\quad + K_2K_3K_4 - \beta(\eta_1K_2K_4 + \tau_1K_3) \\ &= K_1K_2K_4(1 - \mathcal{R}_{i1}^*) + K_1K_3(K_2 + K_4)(1 - \mathcal{R}_{i2}^*) + K_2K_3K_4 - \beta(\eta_1K_2K_4 + \tau_1K_3) \\ D &= K_1K_2K_3K_4(1 - \mathcal{R}_i^*). \end{aligned}$$

The Routh-Hurwitz criteria [19] for the local asymptotic stability in this case are $A > 0, C > 0, D > 0$ and $ABC - C^2 - A^2D > 0$. The first three conditions are satisfied if $\mathcal{R}_i^* < 1$ which implies that $\mathcal{R}_{i1}^* < 1$ and $\mathcal{R}_{i2}^* < 1$ so that $\beta\tau_1 < K_1K_2$ and $\beta\eta_1 < K_1$, respectively. The last condition holds since all terms remaining in the expansion after cancelation are positive. Thus the disease free equilibrium, \mathcal{E}_0^q of model (1) with $q = 1$ is locally asymptotically stable when $\mathcal{R}_i^* < 1$.

It is instructive to note that if $\mathcal{R}_i^* = 1$, the coefficient D of the characteristic equation (15) is zero and so, J_q has a zero eigenvalue. This indicates the occurrence of a bifurcation when $\mathcal{R}_i^* = 1$ which will be investigated using Centre Manifold theory as described in Castillo-Chavez and Song [6, Theorem 4.1] in Subsection 3.4.

The epidemiological interpretation of this result is that MERS-CoV will be eliminated if the initial sizes of the infected sub-populations of the model are in the basin of attraction of the DFE (\mathcal{E}_0^q). However, disease eradication is independent of the initial sizes if the DFE is globally asymptotically stable. The global stability result is established in the following theorem.

Theorem 2 *The DFE (\mathcal{E}_0^q) of model (1) with $q = 1$ is globally-asymptotically stable (GAS) when $\mathcal{R}_i^* < 1$.*

Proof. The proof is based on the approach in [5]. Using the notation in [5], for system (1) with $q = 1$, $X = S, Z = (L, I, Q, J)$, and $X^* = (\frac{\Pi + \alpha}{\mu}, 0)$. Then, the equation of uninfected is

$$\frac{dX}{dt} = F(X, Z) = \Pi + \alpha + \sigma(1 - p)Q - \lambda S - \mu S,$$

and the infected subsystem is

$$\frac{dZ}{dt} = G(X, Z) = \begin{pmatrix} \lambda S - (\tau_1 + \tau_2 + \mu)L \\ \tau_1 L - (\gamma + \nu_1 + \delta_1 + \mu)I \\ \tau_2 L - (\sigma + \mu)Q \\ \gamma I - (\nu_2 + \delta_2 + \mu)J \end{pmatrix}$$

When $L = I = Q = J = 0$ (i.e., $Z = 0$), then $F(X, 0) = (\Pi + \alpha) - \mu S$, and

$$A = D_Z G(X^*, 0) = \begin{pmatrix} \beta\eta_1 - K_1 & \beta & \beta\eta_2 & \beta\eta_3 \\ \tau_1 & -K_2 & 0 & 0 \\ \tau_2 & 0 & -K_3 & 0 \\ 0 & \gamma & 0 & -K_4 \end{pmatrix}$$

is obviously an M-matrix (a matrix whose off diagonal elements are nonnegative).

Next, we have

$G(X, Z) = AZ - \hat{G}(X, Z)$, which implies that

$$\hat{G}(X, Z) = \begin{pmatrix} \beta[\eta_1 L(1 - \frac{S}{N}) + I(1 - \frac{S}{N}) + \eta_2 Q(1 - \frac{S}{N}) + \eta_3 J(1 - \frac{S}{N})] \\ 0 \\ 0 \\ 0 \end{pmatrix}.$$

It is clear that $\hat{G}(X, Z) \geq 0$, since $0 \leq S \leq N$. It is also clear that $X^* = (\frac{\Pi + \alpha}{\mu}, 0)$ is a global asymptotic stable equilibrium of $\frac{dX}{dt} = F(X, 0)$. Thus, by using a result in [5], we conclude that \mathcal{E}_0^q is globally-asymptotically stable when $\mathcal{R}_i^* < 1$. \blacksquare

It follows from Theorem 1 that, model (1) with $q = 1$ has a unique endemic equilibrium if $\mathcal{R}_i^* > 1$.

Now, let \mathcal{E}_0^α and $\hat{\mathcal{E}}_\alpha$ be the disease free and endemic equilibria of model (1), respectively with negligible immigration rate ($\alpha = 0$), then we obtain the following results.

Theorem 3 *The unique DFE, \mathcal{E}_0^α of model (1) with $\alpha = 0$ is globally-asymptotically stable if $\mathcal{R}_i^* < 1$, otherwise unstable.*

Theorem 4 *The unique endemic equilibrium, $\hat{\mathcal{E}}_\alpha$ of model (1) with $\alpha = 0$ is globally-asymptotically stable if $\mathcal{R}_i^* > 1$.*

Hence, the summary of the stability results of the model equilibria is given in Table 2.

3.4 Bifurcation analysis

Here we investigate the existence of bifurcation of model (1) using Centre Manifold theory since the Jacobian matrix J_q for the case when all the immigrants are susceptible has a simple zero eigenvalue when $\mathcal{R}_i^* = 1$ with other eigenvalues having negative real parts as presented in Subsection 3.3. In order to apply such a theory, we make the following change of variables $S = x_1, L = x_2, I = x_3, Q = x_4, J = x_5$, so that we use the vector notation $\mathbf{x} = (x_1, x_2, x_3, x_4, x_5)^T$. Then system (1) with $q = 1$ can be written in the form $\frac{d\mathbf{x}}{dt} = F(\mathbf{x})$ with $f = (f_1, f_2, f_3, f_4, f_5)^T$, such that

$$\begin{aligned} \dot{x}_1 &= \Pi + \alpha + \sigma(1-p)x_4 - \frac{\beta(\eta_1 x_2 + x_3 + \eta_2 x_4 + \eta_3 x_5)}{x_1 + x_2 + x_3 + x_4 + x_5 + x_6} x_1 - \mu x_1, \\ \dot{x}_2 &= \frac{\beta(\eta_1 x_2 + x_3 + \eta_2 x_4 + \eta_3 x_5)}{x_1 + x_2 + x_3 + x_4 + x_5 + x_6} x_1 - (\tau_1 + \tau_2 + \mu)x_2, \\ \dot{x}_3 &= \tau_1 x_2 - (\gamma + \nu_1 + \delta_1 + \mu)x_3, \\ \dot{x}_4 &= \tau_2 x_2 - (\sigma + \mu)x_4, \\ \dot{x}_5 &= \gamma x_3 - (\nu_2 + \delta_2 + \mu)x_5. \end{aligned} \tag{16}$$

The Jacobian matrix of system (16) at \mathcal{E}_0 is the same with J_q as presented in (14). If β is taken as a bifurcation parameter, we obtain from $\mathcal{R}_i^* = 1$ that

$$\beta = \beta^* = \frac{K_1 K_2 K_3 K_4}{\tau_1 K_3 (K_4 + \eta_3 \gamma) + K_2 K_4 (\eta_1 K_3 + \eta_2 \tau_2)}.$$

It can be verified that the Jacobian of (16) at $\beta = \beta^*$ has a right eigenvector associated with zero eigenvalue given by $\mathbf{u} = (u_1, u_2, u_3, u_4, u_5)^T$, with

$$\begin{aligned} u_1 &= \frac{\beta}{\mu} \left(-\eta_1 + \frac{\tau_1}{K_2} + \sigma(1-p) \frac{\tau_2}{K_3} - \frac{\eta_3 \gamma \tau_1}{K_2 K_4} \right) u_2, u_2 = u_2 > 0, u_3 = \frac{\tau_1}{K_2} u_2, \\ u_4 &= \frac{\tau_2}{K_3} u_2, \text{ and } u_5 = \frac{\gamma}{K_4}. \end{aligned} \tag{17}$$

Similarly, the left eigenvalue of $J_q(\mathcal{E}_0)$ associated with zero eigenvalue at $\beta = \beta^*$ is given by $\mathbf{v} = (v_1, v_2, v_3, v_4, v_5)^T$, where

$$v_1 = 0, v_2 = v_2 > 0, v_3 = \frac{\beta}{K_2 K_4} (\gamma \eta_3 - K_4) v_2, v_4 = \frac{\beta \eta_2}{K_3} v_2, v_5 = \frac{\beta \eta_3}{K_4} v_2. \tag{18}$$

To establish the existence of bifurcation, we need to compute a and b as follows. Let F_k be the k^{th} component of F , then as defined in [6]

$$\begin{aligned} a &= \sum_{k,i,j=1}^5 v_k u_i u_j \frac{\partial^2 F_k}{\partial x_i \partial x_j}(\mathcal{E}_0) \\ b &= \sum_{k,i,j=1}^5 v_k u_i \frac{\partial^2 F_k}{\partial x_i \partial x_j \beta^*}(\mathcal{E}_0). \end{aligned} \tag{19}$$

Now, for system (16) the associated non zero partial derivatives of F at the disease free equilibrium are as follows:

$$\begin{aligned}\frac{\partial^2 F_2}{\partial x_2^2} &= -\frac{2\beta^*\eta_1\mu}{\Pi + \alpha}, & \frac{\partial^2 F_2}{\partial x_2 x_3} &= -\frac{\beta^*\mu(\eta_1 + 1)}{\Pi + \alpha} \\ \frac{\partial^2 F_2}{\partial x_2 x_4} &= -\frac{\beta^*\mu(\eta_1 + \eta_2)}{\Pi + \alpha}, & \frac{\partial^2 F_2}{\partial x_2 x_5} &= -\frac{\beta^*\mu(\eta_1 + \eta_3)}{\Pi + \alpha}.\end{aligned}\quad (20)$$

It follows from (19) and (20) that

$$a = -\frac{\beta\mu u_2 v_2}{\Pi + \alpha} \left(2\eta_1 u_2 + \frac{\tau_1(\eta_1 + 1)}{K_2} + \frac{\tau_2(\eta_1 + \eta_2)}{K_3} + \frac{\gamma(\eta_1 + \eta_3)}{K_4} \right), \quad (21)$$

which is negative, and for the sign of b , it is associated with the following non zero partial derivatives of F

$$\begin{aligned}\frac{\partial^2 F_1}{\partial x_2 \partial \beta} &= -\eta_1, & \frac{\partial^2 F_1}{\partial x_3 \partial \beta} &= -1, & \frac{\partial^2 F_1}{\partial x_4 \partial \beta} &= -\eta_2, & \frac{\partial^2 F_1}{\partial x_5 \partial \beta} &= -\eta_3 \\ \frac{\partial^2 F_2}{\partial x_2 \partial \beta} &= \eta_1, & \frac{\partial^2 F_2}{\partial x_3 \partial \beta} &= 1, & \frac{\partial^2 F_2}{\partial x_4 \partial \beta} &= \eta_2, & \frac{\partial^2 F_2}{\partial x_5 \partial \beta} &= \eta_3.\end{aligned}\quad (22)$$

It follows from the expression of b in (19) and the derivatives in (22) that

$$b = \left(\eta_1 u_2 + \frac{\tau_1}{K_2} + \frac{\tau_2 \eta_2}{K_3} + \frac{\gamma \eta_3}{K_4} \right) v_2 > 0. \quad (23)$$

We obtain from the computations of a and b above that a is negative and b is positive. Thus, using Theorem 4.1 (iv) in [6], we establish the following result

Theorem 5 *The system of equations (1) with $q = 1$ exhibits a transcritical bifurcation at \mathcal{E}_0 if the bifurcation parameter $\beta^* = \frac{K_1 K_2 K_3 K_4}{\tau_1 K_3 (K_4 + \eta_3 \gamma) + K_2 K_4 (\eta_1 K_3 + \eta_2 \tau_2)}$ or equivalently $\mathcal{R}_i^* = 1$.*

3.5 The impact of quarantine/isolation/immigration

In this section, the impact of quarantine and isolation on the transmission dynamics of MERS-CoV is investigated via a threshold analysis approach on the invasion threshold parameter, \mathcal{R}_i . This is carried out in terms of the parameters associated with quarantine of latent immigrants τ_2 and the isolation of individuals with disease symptoms γ . More precisely, the threshold \mathcal{R}_i is considered as a function of τ_2 and γ . For the case of the quarantine of latently infected individuals, the rate of change of \mathcal{R}_i with respect to τ_2 is as follows:

$$\frac{\partial \mathcal{R}_i}{\partial \tau_2} = \frac{\beta \eta_2}{K_1 K_2} - \frac{\beta [K_2 K_4 (\eta_1 K_3 + \eta_2 \tau_2) + \tau_1 K_3 (K_4 + \eta_3 \gamma)]}{K_1^2 K_2 K_3 K_4}. \quad (24)$$

Table 2: Summary of the stability results of the full model and its two special cases.

Equilibrium	Invasion threshold	Stability
$\hat{\mathcal{E}}$	$\mathcal{R}_i \leq 1$	GAS
\mathcal{E}_0^q	$\mathcal{R}_i^* < 1$	LAS/GAS
\mathcal{E}_0^α	$\mathcal{R}_i^* < 1$	LAS/GAS
$\hat{\mathcal{E}}_q$	$\mathcal{R}_i^* > 1$	GAS
$\hat{\mathcal{E}}_\alpha$	$\mathcal{R}_i^* > 1$	GAS

Let us define from (24) that

$$\begin{aligned} \eta_2^* &= \frac{\eta_1 K_2 K_3 K_4 + \tau_1 K_3 (K_4 + \eta_3 \gamma)}{K_2 K_4 (K_1 - \tau_2)} \\ &= \frac{\eta_1 K_2 K_3 K_4 + \tau_1 K_3 (K_4 + \eta_3 \gamma)}{K_2 K_4 (\tau_1 + \mu)}, \end{aligned} \quad (25)$$

since $K_1 = \tau_1 + \tau_2 + \mu$. Therefore,

$$\frac{\partial \mathcal{R}_i}{\partial \tau_2} \leq 0 \text{ if and only if } \eta_2 \leq \eta_2^*.$$

Thus, this threshold parameter will be a decreasing function of the quarantine parameter τ_2 , resulting in a decrease of disease burden (new infections and mortality) if the relative infectiousness of quarantine individuals η_2 does not exceed its associated threshold η_2^* . By contrast, if $\eta_2 > \eta_2^*$, then the use of quarantine of latent immigrants will increase the threshold parameter (\mathcal{R}_i) and so, increase disease burden. In this case, the use of quarantine is detrimental to a community. The result is summarized as follows.

Proposition 1 *The use of quarantine of the latent immigrants will have positive (negative) impact in a community if $\eta_2 \leq \eta_2^*$.*

Similarly, the rate of change of \mathcal{R}_i with respect to isolation parameter γ is given by

$$\begin{aligned} \frac{\partial \mathcal{R}_i}{\partial \gamma} &= \frac{\beta [K_4 (\eta_1 K_3 + \eta_2 \tau_2) + \tau_1 \eta_3 K_3]}{K_1 K_2 K_3 K_4} \\ &\quad - \frac{\beta [K_2 K_4 (\eta_1 K_3 + \eta_2 \tau_2) + \tau_1 K_3 (K_4 + \eta_3 \gamma)]}{K_1 K_2^2 K_3 K_4}. \end{aligned} \quad (26)$$

We obtain from (26) that

$$\eta_3^* = \frac{K_4}{\delta_1 + \nu_1 + \mu} = \frac{\delta_2 + \nu_2 + \mu}{\delta_1 + \nu_1 + \mu}, \quad (27)$$

so that

$$\frac{\partial \mathcal{R}_i}{\partial \gamma} \leq 0 \text{ if and only if } \eta_3 \leq \eta_3^*.$$

It follows that, \mathcal{R}_i will be a decreasing function of the isolation parameter γ and hence decrease disease burden if $\eta_3 < \eta_3^*$. It will be an increasing function of γ , on one hand, when $\eta_3 > \eta_3^*$. In such a case, the use of isolation will have a detrimental impact in a community. This result is summarized in the following proposition.

Proposition 2 *The use of isolation of infectious individuals will have positive (negative) impact in a community if $\eta_3 \leq \eta_3^*$.*

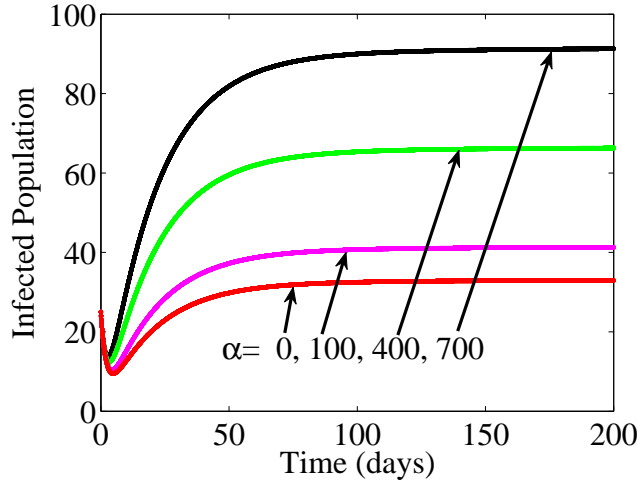
These results (Propositions 1 and 2) are illustrated numerically in section 3.5.1 below.

It worthies mentioning here that, the critical parameters η_2^* and η_3^* as defined in (25) and (27), respectively, remain the same for the case when either all immigrants are susceptibles ($q=1$) or the immigration rate is negligible, $\alpha = 0$. Hence, the results in Propositions 1 and 2 also hold true for such two cases.

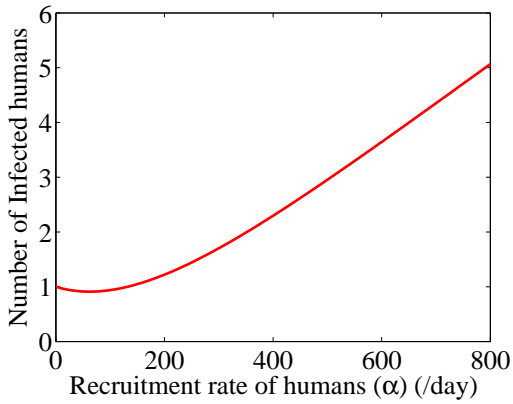
To explore the impact of influx of immigrants into the susceptible and latent compartments on the dynamics of MERS-CoV, we use numerical experiment to vary different values of the immigration rate (α), while keeping all other model parameters fixed. In fact, the numerical simulations reveal that the number of infected individuals increases with increasing values of α . As depicted in Figure 3(a), when the influx increases from 0 to 700, the infected individuals increases from 30 to 90 as well. It also shows that the prevalence is very low (ranges between 10 to 14) and the steady state value I is also very small, whereas, for $0 \leq \alpha \leq 100$, it ranges between 32 to 42 about, and if $\alpha = 700$ then $I(200)$ is less than 100. Moreover, Figure 3(b) shows more clearly that the number of infected individuals increases with increasing value of α , while Figure 3(c) indicates that, there might be a critical value of α above which the disease prevalence decreases due to the positive impact of quarantine and isolation (Propositions 1 and 2) so that the disease will die out with time. However, eradication of MERS-CoV in a community is feasible if quarantine and isolation is combined with a high reduction of immigration rate.

3.5.1 Numerical simulations

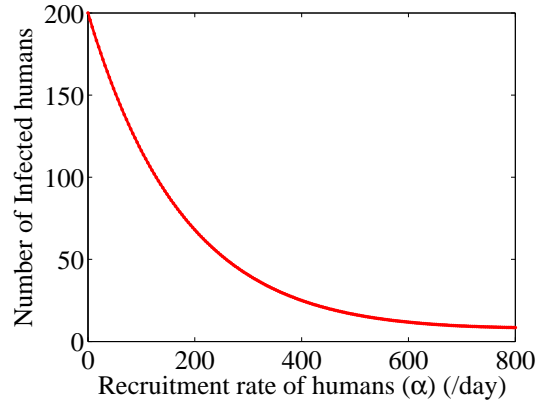
The numerical simulations in Figure 4(a) is depicting the result of Proposition 1 in which the invasion threshold parameter \mathcal{R}_i , is a decreasing function of the quarantine parameter τ_2 , whenever the modification parameter for quarantine is less than a critical value $\eta_2^* = 0.3118$. Thus, for values of $\eta_2 = 0.017, 0.25$, less than η_2^* , the cumulative new cases of infection decreases from about 27,000 to 16,500 individuals. However, for $\eta_2 = 0.5, 0.75$, greater than the critical value, the cumulative new cases increases from about 28,500 to 38,500 individuals.



(a)



(b)



(c)

Figure 3: The simulation showing the impact of immigration on the number of infected individuals using parameter values as in Table (3). (a) The infected humans increases with increasing influx of immigrants. (b) indicates that the infected humans increases to a certain level. (c) reveals that there is a critical immigration rate above which the infected humans decreases.

Similarly, Figure 4(b) illustrates the result of Proposition 2, the impact of isolation in controlling the disease, in which the control reproduction number \mathcal{R}_i , is a decreasing function of the isolation parameter γ , whenever the modification parameter for quarantine is less than a critical value $\eta_3^* = 0.1087$. Thus, for values of $\eta_3 = 0.0001$ to 0.017 , less than η_3 , the cumulative new cases of infection decreases from about 18,500 to 16,500 individuals. However, for $\eta_3 = 0.25$ to 0.55 , greater than the critical value, the cumulative new cases increases from about 26,500 to 32,500 individuals.

Table 3: Parameter values for the model (1)

Parameter	Nominal value	Reference
Π	400 per day	Assumed
β	0.25 per day	Assumed
α	≥ 0 per day	Assumed
μ	0.0000374 per day	[11]
η_1	(0.001, 0.65)	Assumed
η_2	(0.013, 0.78)	Assumed
η_3	(0.002, 0.65)	Assumed
γ	(0.00138, 0.05) per day	[2, 8]
σ	(0.00138, 0.025) per day	[2, 8]
ν_1	(0.0018, 0.0028)per day	[2, 25]
ν_2	(0.0012, 0.0018)per day	[2, 8, 25]
τ_1	(0.0018, 0.0028)per day	[2]
τ_2	(0.0012, 0.0018)per day	[2, 8]
δ_1	(0.0337, 0.26) per day	[2]
δ_2	(0.26, 0.5) per day	[2]
p	[0, 1]	Assumed
q	[0, 1]	Assumed

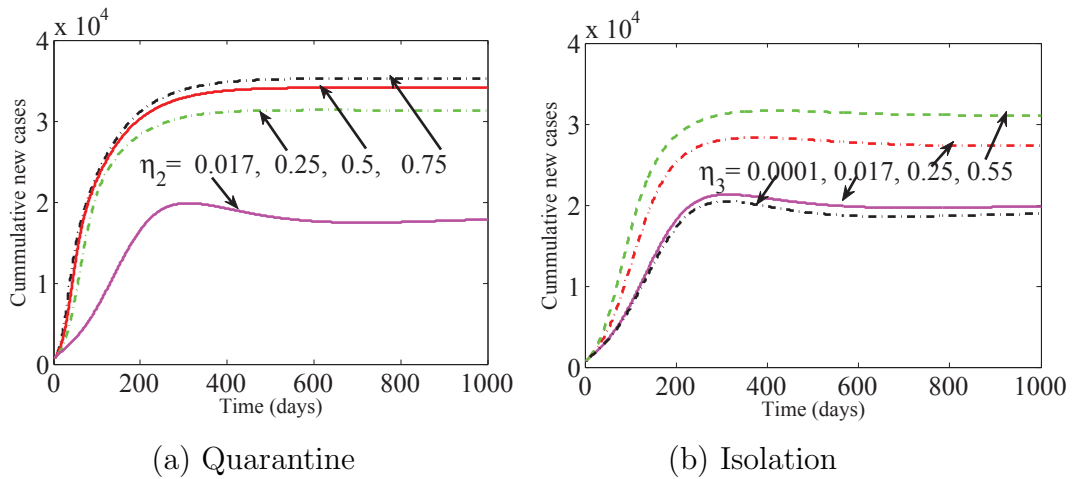


Figure 4: The simulations showing the impact of quarantine and isolation in controlling the infection with parameter values as in Table (3). (a) Quarantine with critical value, $\eta_2^* = 0.3118$. (b) Isolation with critical parameter $\eta_3^* = 0.1087$

4 Discussion and Conclusion

A new deterministic model for the spread of the Middle East Respiratory Syndrome coronavirus in a community with quarantine and isolation as control strategies is formulated and rigorously analyzed. We notice that the presented model does not have disease free equilibrium point due to constant in flux of the latent immigrants and so, there is an endemic persistence of MERS-CoV depending on the invasion threshold parameter \mathcal{R}_i , immigration rate as well as the epidemiological status of the immigrants. In fact, if the immigration rate $\alpha > 0$ and fraction of susceptible immigrants $q \in [0, 1)$, then the disease invades the population for all values of \mathcal{R}_i . On the other hand, endemic persistence is only possible if either immigration rate is negligible or when all immigrants are susceptible provided $\mathcal{R}_i^* > 1$. Stability analysis is carried out for the full model and these two immigration scenarios. We showed numerically that this equilibrium point is a global attractor when $\mathcal{R}_i^* \leq 1$, see Figure 2. For the case when all the immigrants are susceptible, we proved the global asymptotic stability of the associated disease free equilibrium (\mathcal{E}_0^q) if the threshold parameter $\mathcal{R}_i^* < 1$. Such a stability result hold true for the case when the immigration rate is negligible, $\alpha = 0$ and the result follows easily from the first scenario. The existence and stability of endemic equilibrium for these scenarios follows from that of the full model.

In order to complete our investigation, we assess the impact of quarantine and isolation via a threshold analysis approach. Indeed, we showed that quarantine of latent immigrants will decrease the burden of the epidemics (new infections), if the rate of the relative infectiousness of quarantined individuals does not exceed certain threshold quantity, η_2^* . In a similar note, an isolation of infected individuals using intensive care units of hospitals, will have positive impact on the burden of the epidemics (new

infections and mortality due to disease) by reducing the threshold parameter, if the relative infectiousness of isolated individuals does not exceed certain threshold quantity, η_3^* . These results are summarized in Propositions 1 and 2 and numerically supported by Figure 4.

Furthermore, numerical simulations of the model reveal that the influx of susceptible and latent immigrants increase the number of infected individuals. In fact, one can observe from Figure 3(a) that if the influx of these immigrants increases from 0 to 700, the number of infected individuals rises from 30 to 90. Despite such an effect of the immigration rate (α), the positive impact of isolation and quarantine drastically reduces the disease prevalence. As shown in Figure 3(a), the prevalence is very low (ranges between 10 to 14) and the steady state I is also very small. While for $0 \leq \alpha \leq 100$ it ranges between 32 to 42 about, and if $\alpha = 700$ then $I(200)$ is less than 100. Moreover, Figure 3(b) shows more clearly that the number of infected individuals increases as the immigration rate increases, whereas, Figure 3(c) indicates that, there might be a critical value of α above which the number of infectious humans decreases perhaps, due to the positive impact of quarantine and isolation (Propositions 1 and 2) so that the disease will die out with time. It is worthy of mention that, most of the parameter values used are obtained from some related literature as presented in Table 3. The ranges of such parameter values are chosen from minimum and maximum as presented in such existing works for the sake of consistency. While we assumed the values of the parameters (p, q and η_i for $i = 1, 2, 3$) in the interval $[0, 1]$ since each of such parameters is either a fraction of humans or a fraction that account for the assumed reduction in infectiousness of individuals in the latent, quarantined and isolated compartments. Moreover, the values of the recruitment rate Π and the effective contact rate β are assumed in relation to their values used for SARS model in [11].

In conclusion, we showed using a deterministic model that MERS-CoV can be controlled by quick isolation or monitoring close contacts with the patients infected by MERS-CoV and quarantine of suspected latently infected individuals. This is similar to the finding in [27]. In addition, reducing the influx of immigrants plays a significant role in decreasing the number of infected individuals when the recruitment rate of immigrants is below a certain critical value. This is a value of α below which the prevalence is high. However, community-wide eradication of MERS-CoV is feasible when quarantine and isolation are combined with high reduction of the immigration rate into a community.

Acknowledgements

The authors acknowledged the support of South African DST/NRF SARChI chair on Mathematical Models and Methods in Bioengineering and Biosciences (N00317). They are also indebted to the two anonymous Reviewers and the Handling editor for their

constructive comments and suggestions which have enhanced the paper.

References

- [1] A. N. Alagaili, T. Briese, N. Mishra, V. Kapoor, S. C. Sameroff, E. de Wit, V. J. Munster, L. E. Hensley, I. S. Zalmout, A. Kapoor, J. H. Epstein, W. B. Karesh, P. Daszak, O. B. Mohammed, W. I. Lipkin, . Middle East Respiratory Syndrome Coronavirus Infection in Dromedary Camels in Saudi Arabia, *mBio* **5** (2) (2014), e00884–14, doi:10.1128/mBio.00884–14.
- [2] A. Assiri, A. McGeer, T. M. Perl, C. S. Price, A. A. Al Rabeeah, D. A. T. Cummings, Z. N. Alabdullatif, M. Assad, A. Almulhim, H. Makhdoom, H. Madani, R. Alhakeem, J. A. Al-Tawfiq, M. Cotten, S. J. Watson, P. Kellam, A. I. Zumla, and Z. A. Memish, Hospital outbreak of Middle East Respiratory Syndrome Coronavirus, *N Engl J Med* **369** (5) (2013) 407–416.
- [3] A. Bermingham, M. A. Chand, C. S. Brown, E. Aarons, C. Tong, C. Langrish, K. Hoschler, K. Brown, M. Galiano, R. Myers, R. G. Pebody, H. K. Green, N. L. Boddington, R. Gopal, N. Price, W. Newsholme, C. Drosten, R. A. Fouchier and M. Zambon, Severe respiratory illness caused by a novel coronavirus, in a patient transferred to the United Kingdom from the Middle East. *Euro Surveill*, **17** (40) (2012).
- [4] F. Brauer, P. van den Driessche, Models for the transmission of disease with immigration of infectives, *Math. Biosci.* **171**, 2001 143-154.
- [5] C. Castillo-Chavez, Z. Feng and W. Huang (2002), On the computation of \mathcal{R}_0 and its role on global stability. In: C. Castillo-Chavez, S. Blower, P. van der Driessche, D. Kirschner, and A. Yakubu (eds) *Mathematical approaches for emerging and reemerging infectious diseases: an introduction*, Springer (2002) 261–274.
- [6] C. Castillo-Chavez, B. Song, Dynamical models of tuberculosis and their applications, *Math. Biosci. Engineer.* **1**(2) (2004) 361–404
- [7] S. Cauchemez, C. Fraser, M. D. V. Kerkhove, C. A. Donnelly, S. Riley, A. Rambaut, V. Enouf, S. van der Werf, N. M. Ferguson, Middle East respiratory syndrome coronavirus: quantification of the extent of the epidemic, surveillance biases, and transmissibility, *Lancet Infect Dis*, **14** (2014) 50-56.
- [8] CIDRAP Center for infectious diseases research and policy, University of Minnesota (2014) [http : //www.cidrap.umn.edu/news-perspective/2013/09/eight-new-saudi-cases-push-global-mers-total-130](http://www.cidrap.umn.edu/news-perspective/2013/09/eight-new-saudi-cases-push-global-mers-total-130) (Accessed September 14 2014).

- [9] R. J. de Groot, S. C. Baker, R. S. Baric, C. S. Brown, C. Drosten, L. Enjuanes, R. A. M. Fouchier, M. Galiano, A. E. Gorbalenya, Z. A. Memish, S. Perlman, L. L. M. Poon, E. J. Snijder, G. M. Stephens, P. C. Y. Woo, A. M. Zaki, M. Zambon and J. Ziebuhr, Middle East Respiratory Syndrome Coronavirus (MERS-CoV): Announcement of the Coronavirus Study Group. *J. Virol.*, **87**(14) (2013) 7790–7792.
- [10] Gloval overview of an emerging novel coronavirus (MERS-CoV), World Health Assembly (2013).
- [11] A. B. Gumel, S. Ruan, T. Day, J. Watmough, F. Brauer, P. van den Driessche, D. Gabrielson, C. Bowman, M. E. Alexander, S. Ardal, J. Wu and B. M. Sahai, Modelling strategies for controlling SARS outbreaks, *Proc. R. Soc. Lond. B* **271** (2004) 2223–2232.
- [12] H. Guo, M. Y. Li, Impacts of migration and immigration on disease transmission dynamics in heterogeneous populations, *Discrete Contin. Dyn. Syst., Ser. B*, **17**(7) (2012) 2413–2430.
- [13] B. L. Haagmans, S. H. S. Al Dhahiry, C. B. E. M. Reusken, V. S. Raj, M. Galiano, R. Myers, G.-J. Godeke, M. Jonges, E. Farag, A. Diab, H. Ghobashy, F. Alhajri, M. Al-Thani, S. A. Al-Marri, H. E. Al Romaihi, A. Al Khal, A. Bermingham, A. D. M. E. Osterhaus, M. M. AlHajri and M. P. G. Koopmans, Middle East respiratory syndrome coronavirus in dromedary camels: an outbreak investigation, *Lancet Infect Dis*, **14** (2014) 140–45.
- [14] J.K. Hale, S.M.V. Lunel, *Introduction to functional differential equations*, Springer-Verlag, Berlin, Heidelberg, New York, 1993.
- [15] HealthMap organization (2014). [http : //www.healthmap.org/en/](http://www.healthmap.org/en/) (Accessed March 14 2014).
- [16] M. G. Hemida1, R. A. Perera, P. Wang, M. A. Alhammadi, L. Y. Siu, M. Li, L. L. Poon, L. Saif, A. Alnaeem and M. Peiris, Middle East Respiratory Syndrome (MERS) coronavirus seroprevalence in domestic livestock in Saudi Arabia, 2010 to 2013, *Euro Surveill*, **18** (50) (2013) pii=20659. Available online: [http : //www.eurosurveillance.org/](http://www.eurosurveillance.org/).
- [17] K. Kupperschmidt, Researchers scramble to understand camel connection to MERS, *SCIENCE*, **341** (2013).
- [18] J. Lee, G. Chowell, and E. Jung, A dynamic compartmental model for the middle east respiratory syndrome outbreak in the republic of korea: A retrospective

- analysis on control interventions and superspreading events, *Journal of theoretical biology*, **408** (2016) 118–126.
- [19] P. Lancaster, *Theory of Matrices*, New York, (1969).
- [20] P. M. Penttinen, K. Kaasik-Aaslav, A. Friaux, A. Donachie, B. Sudre, A. J. Amato-Gauci, Z. A. Memish, D. Coulobmier, Taking stock of the first 133 MERS coronavirus cases globally Is the epidemic changing? *Euro Surveill*, **18** (39) (2013) 1–5.
- [21] R. A. Perera, P. Wang, M. R. Goma, R. El-Shesheny, A. Kandeil, O. Bagato, L. Y. Siu, M. M. Shehata, A. S. Kayed, Y. Moatasim, M. Li, L. L. Poon, Y. Guan, R. J. Webby, M. A. Ali, J. S. Peiris and G. Kayali (2013). Seroepidemiology for MERS coronavirus using microneutralisation and pseudoparticle virus neutralisation assays reveal a high prevalence of antibody in dromedary camels in Egypt, June 2013. *Euro Surveill*, **18** (36):pii=20574. Available online: <http://www.eurosurveillance.org/ViewArticle.aspx?ArticleId=20574>.
- [22] C. B. Reusken, M. Ababneh, V. S. Raj, B. Meyer, A. Eljarah, S. Abutarbush, G. J. Godeke, T. M. Bestebroer, I. Zutt, M. A. Miller, B. J. Bosch, P. J. Rottier, A. D. Osterhaus, C. Drosten, B. L. Haagmans and M. P. Koopmans, Middle East Respiratory Syndrome coronavirus (MERS-CoV) serology in major livestock species in an affected region in Jordan, June to September 2013, *Euro Surveill*, **18** (50) (2013) pii=20662. Available online: <http://www.eurosurveillance.org/ViewArticle.aspx?ArticleId=20662>.
- [23] M.A Safi, A.B. Gumel, Mathematical analysis of a disease transmission model with quarantine, isolation and an imperfect vaccine, *Computers and Mathematics with applications*, **61** (2011) 3044–3070.
- [24] M.A Safi, A.B. Gumel, Qualitative study of a quarantine/isolation model with multiple disease stages, *Applied Mathematics and Computation* **218** (2011) 1941–1961.
- [25] World Health Organization (WHO) (2014). Global Alert and Response (GAR): Middle East respiratory syndrome coronavirus (MERS-CoV) update http://www.who.int/csr/don/20140411_mers/en/ (accessed April 21, 2014).
- [26] World Health Organization (WHO). Global Alert and Response (GAR): novel coronavirus infection <http://www.who.int/csr/don/20130801/en/index.html> (accessed Aug 1, 2014).

- [27] Z.-Q. Xia, J. Zhang, Y.-K. Xue, G.-Q. Sun, and Z. Jin, Modeling the transmission of middle east respiratory syndrome corona virus in the republic of korea, *PloS one*, **10** (2015), p. e0144778.
- [28] A. M. Zaki, S. van Boheemen, T. M. Bestebroer, A. D.M.E. Osterhaus, and R. A.M. Fouchier, Isolation of a Novel Coronavirus from a Man with Pneumonia in Saudi Arabia. *N Engl J Med*, **367** (2012) 1814–1820.